Global Journal of Pure and Applied Chemistry Research, 13, (1), 1-11, 2025
Print ISSN: ISSN 2055-0073(Print),
Online ISSN: ISSN 2055-0081(Online)
Website: https://www.eajournals.org/
Publication of the European Centre for Research Training and Development-UK

Nanotechnical Synthesis, Fourier Trandformed Infrared Study of Biogenic Siver Nanoparticles (Agnps) From *Moringer Oleifera* Leave Extract for Photodegradation of Methylene Blue Under Visible Light Irradiation

[2] Edmond Moses [1]Bala Adamu Thliza, [2]Abdulrahaman Hudu, [2]Hosea Sarah and [1]Irfan Zaheer Khan

1. Department of pure and Applied Chemistry, University of Maiduguri Borno State PMB 1069 Borno State Nigeria.
2. Department of Chemistry Nigeria Army University Biu. No. 1 Biu - Gombe Road, P.M.B, 1500 Biu, Borno State Nigeria

doi: https://doi.org/10.37745/gjpacr.2023/vol13n1111 Published February 14, 2024

Citation: Moses E., Thliza B.A., Hudu A., Sarah H., and Khan I.Z. (2025) Nanotechnical Synthesis, Fourier Trandformed Infrared Study of Biogenic Siver Nanoparticles (Agnps) From Moringer Oleifera Leave Extract for Photodegradation of Methylene Blue Under Visible Light Irradiation, *Global Journal of Pure and Applied Chemistry Research*, 13, (1), 1-11

Abstract: *The synthesized AgNPs successfully degraded methylene blue dye, showcasing their potential as an eco-friendly alternative for dye remediation in wastewater treatment. This study highlights the viability of plant-mediated nanoparticle synthesis as a green method that minimizes harmful chemicals, aligns with environmental safety, and supports sustainable practices. Future research could focus on optimizing reaction conditions, scaling up production, and exploring the long-term stability and reusability of these nanoparticles in industrial applications.*

Keywords*:* Nanotechnical Synthesis, Fourier Trandformed, Biogenic Siver Nanoparticles (AgNPs), Moringer Oleifera Leave, Photodegradation, Methylene Blue, Visible Light Irradiation

INTRODUCTION

Photo catalysts are important materials that provide a relatively simple means for the conversion of light energy including (solar energy) for use in oxidation and reduction process. They utilize light energy (*hv*) to carry out oxidation and reduction reactions. When irradiated with light energy, an electron (e^-) is excited from the valence band (VB) to the conduction band (CB) of Photo catalysts leaving a photogenerated hole (h^+). The produced e^- and h^+enable oxidation and reduction processes to occur. When photocatalytic process takes place in aqueous solutions, water and

hydroxide ions react with photogenerated h^+ to form hydroxyl radicals (*OH) as the primary oxidant in the photocatalytic oxidation of organic compounds (Coa *et al.,* 2007).
Silver nanoparticles has been applied as a visible light responsive photocatalysts for the remediation of hazardous wastes, contaminated groundwater and control of toxic air contaminants (Jadhav *et al.,* 2010).

To enhance the photocatalytic activity of the silver nanoparticles, several methods have been proposed for its synthesis with unique size dependent, physical and chemical properties. Various composites of silver oxide, Ag/TiO_2, Ag/ZnO e.t.c have also been synthesized and their photocatalytic activity is often higher than that of the bare silver (Cao *et al.,* 2007).

Metal nanoparticles are among the most researched due to their unique electronic, magnetic, and optical properties. They include gold (Au), silver (Ag), platinum (Pt), and iron oxide nanoparticles. For instance, gold nanoparticles are highly valued for their stability and biocompatibility, making them useful in biomedical applications such as drug delivery and diagnostics (Gurav *et al.,* 2020). Similarly, silver nanoparticles are widely used for their antimicrobial properties and are incorporated into medical devices, textiles, and packaging materials (Rai *et al.,* 2014).

Metal oxide nanoparticles include compounds like titanium dioxide (TiO_2), zinc oxide (ZnO), and iron oxide (Fe_3O_4). These nanoparticles are primarily applied in environmental protection, catalysis, and as sensors. Titanium dioxide nanoparticles are notably used in sunscreen for their UV-filtering properties and in Photocatalysis for environmental remediation (Zhang *et al.,* 2018). Zinc oxide nanoparticles also exhibit strong antibacterial properties, making them useful in coatings and biomedical fields (Espitia *et al.,* 2012).

Biological Methods
Biological methods, or "green synthesis," involve the use of biological entities like plants, bacteria, or fungi to synthesize nanoparticles. This method is environmentally friendly and can lead to the production of biocompatible nanoparticles. For example, plant extracts have been successfully used to synthesize gold and silver nanoparticles (Iravani, 2011). Green synthesis methods are gaining popularity due to their low toxicity and eco-friendliness.

Biological Effects of *Moringaoleifera*
The bioactive compounds (Figure 1) present in *Moringaoleifera*confer properties associated with disease prevention and treatment, such as antimicrobial, anti-inflammatory, anticancer, antidiabetic, antioxidant, hepatoprotective and cardioprotective (Koul and Chase, 2015). Primary and secondary metabolites may also be involved in these applications. Primary metabolites are proteins, polysaccharides and lipids involved in physiological functions. Among them, polysaccharides and fibres are the main compounds showing positive effects on chronic diseases such as cancer, cardiovascular diseases, diabetes and obesity. On the other hand, secondary metabolites are minor molecules, such as phenolic compounds, halogenated compounds, sterols,

terpenes and small peptides. Most of the phytochemicals reported in *Moringaoleifera*offer potential in the prevention and treatment of diseases. The anti-inflammatory effect is due to the content of flavonoids, alkaloids, tannins and glycosides, among which quercetin appears to inhibit NF-KB activation, producing an antiinflammatory effect (Das, *et al.,* 2013).

MATERIALS AND METHODS

Materials and equipment

1) Silver nitride (Analytical grade, BDH Chemical England)
2) Petroleum ether (Analytical grade, BDH Chemical England)
3) Moringa leave
4) Methylene Blue
5) Conical Flask (500ml, 2000ml) Pyrex.
6) Beaker (5000ml) Pyrex
7) Measuring Cylinder (1000ml, 500ml)
8) Spatula.
9) Filter paper.
10) Funnel.
11) Water Bath.
12) Glass Rod Stirrer.

Sample preparation (Moringa Extracts)

The grounded moringa leave was weighed 50 grams and transferred in to 500 Ml beaker containing 200 mL distilled water, boiled for a n hour to collected an extract which was left undisturbed for 20 minutes, filtered through whatman filter paper under a vacuum condition. The filtered sample was refrigerated at 4 ^{o}C to maintain accuracy and effectiveness in the result for further experiment (Sathyavathhi, *et al.,* 2011)

Green Synthesis of Silver Nanoparticles

10 mL of the Moringa oleifera leaf extract was mixed with 90 mL of the 1 mM silver nitrate solution. The mixture was stirred using a magnetic stirrer for uniform mixing. (Girish, 2011).
The reaction mixture was heated to 70 °C to facilitate the reduction of silver ions (Ag^{+}) to silver nanoparticles (Ag^{0}). The reaction was observed over time (20 min) for a change in color.The reduction of silver ions by the leaf extract was confirmed by a color change from light yellow to dark brown. This change indicated the formation of silver nanoparticles, which occurs due to the surface plasmon resonance (SPR) effect of the nanoparticles (Song & Kim, 2009).

Photo-degradation of Methylene Blue Solution

100 ml of solution of methylene blue solution was taken from the stock solution, put in a beaker; 0.1 g of Photocatalysts Ag added. The suspension was kept in a dark at room temperature with

continuous stirring using magnetic stirrer. After an hour in the dark, the suspension was then irradiated with 300 W halogen lamp. An aliquot of 5 ml was taken from the beaker at interval of 20 minutes for 1 hour, the catalysts were filtered then analysed using UV-Vis Spectrophotometer to evaluate the photocatalytic degradation. Same procedure was repeated for silver variations (0.2g, 0.3, 0.4, and 0.5)

RESULT AND DISCUTION

Synthesis of silver Nanoparticles;

Formation of Ag NPs was easily noticed due to changes in color of the solution. The color changes arise due to excitation of surface plasmon resonance in the metal nanoparticles indicating the formation of AgNPs. When 10 ml of Moringa oleifera extract was added to 90ml of 1mM solution of $AgNO_3$ while stiring and heating (70 ^{0}C) for 20 minutes,the reaction mixture changed its color from pale yellow to brown indicating the formation of AgSNPs.

FOURIER TRANSFORM INFRARED SPECTROSCOPY (FTIR)

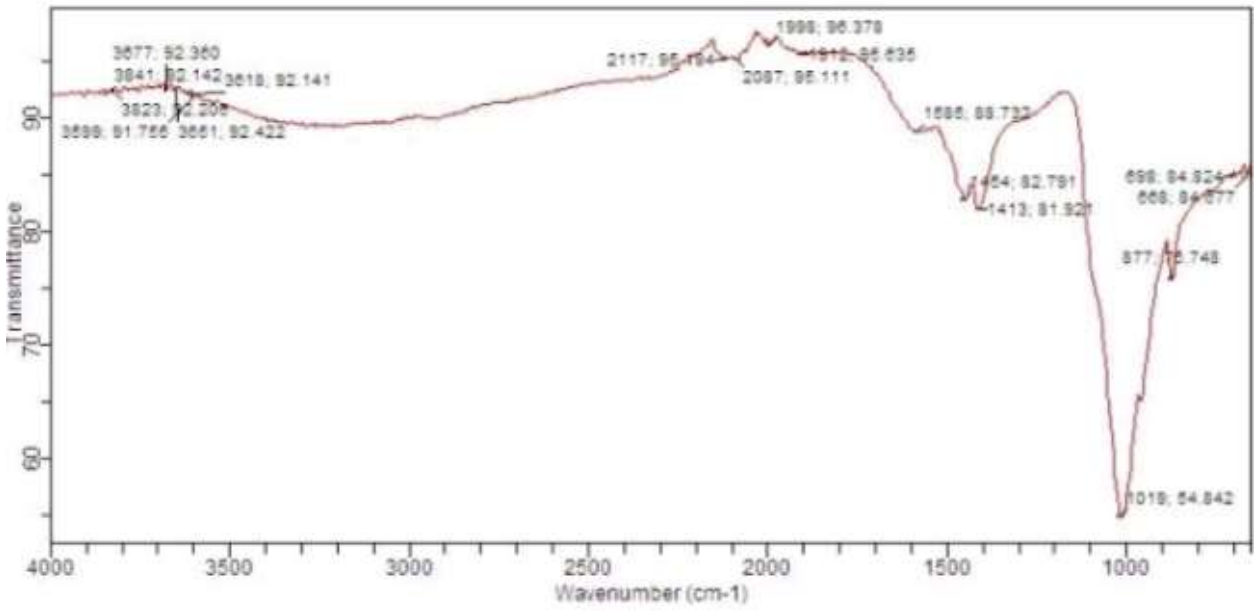

Fig 1. FTIR Spectra

The FTIR analysis is used to identify the functional groups present in the sample, which can help understand the interactions between the nanoparticles and the biomolecules from the plant extract that act as reducing and capping agents during synthesis.

The broad band around 3677-3623 cm^{-1} corresponds to O-H stretching vibrations, which are characteristic of hydroxyl groups (OH) present in alcohols or phenols. These groups are commonly

found in plant extracts, where polyphenols, flavonoids, and other alcohol-based compounds can act as reducing agents to synthesize silver nanoparticles. The peak indicates the presence of biomolecules that stabilize the nanoparticles.

Similar results have been reported in studies involving plant-mediated synthesis of AgNPs, such as those by Nayak *et al., 2015,* where broad peaks in this region were attributed to hydroxyl groups in polyphenolic compounds.

Peaks around ~2100-2000 cm^{-1} (C≡C and C≡N Stretching):The peak at 2117 cm^{-1} may indicate the presence of alkynes (C≡C) or nitriles (C≡N), though these are less commonly reported in plant extracts. This could be due to minor bimolecular components or impurities involved in the nanoparticle capping process.

The peak at 1656 cm^{-1} is typically associated with the C=O stretching of amides (Amide I), proteins, or carbonyl groups from other biomolecules. These functional groups indicate the involvement of proteins or enzymes from the Moringa oleifera leaf extract in the reduction and stabilization of the nanoparticles.

This is in line with research by Shankar *et al.2014,* where similar peaks in the 1650-1660 cm^{-1} range were reported, suggesting the presence of amide groups in the protein capping the silver nanoparticles.

Peak at ~1384 cm^{-1} (C-H Bending or NO2 Symmetric Stretching): This peak could be due to C-H bending vibrations from alkanes or nitrate groups. Plant extracts contain several hydrocarbons and nitrate-like compounds, which could explain the presence of this peak.

The strong absorption band at 1016 cm^{-1} is assigned to C-O stretching vibrations, which are characteristic of alcohols, ethers, or carbohydrates. The presence of such groups suggests the role of polysaccharides or sugars from the plant extract, which help in stabilizing the nanoparticles.
Other Minor Peaks around 877 cm^{-1} and 698 cm^{-1} could be attributed to out-of-plane bending of aromatic C-H bonds, indicating the presence of aromatic compounds. These compounds are common in plant-derived biomolecules, especially flavonoids and phenolic acids, which can reduce and stabilize nanoparticles.

Anandalakshmi *et al. 2016* reported strong peaks around 1640 cm^{-1} for C=O stretching and broad bands around 3300 cm^{-1} for O-H stretching when using Moringa oleifera extract for AgNPs synthesis . This suggests that plant-derived compounds like proteins, polysaccharides, and polyphenols act as reducing and capping agents during nanoparticle formation.

The presence of hydroxyl and carbonyl groups in the FTIR spectrum is consistent with findings by Singh *et al. 2015,* where FTIR analysis of AgNPs synthesized using Azadirachta indica extract

showed similar peaks, indicating the involvement of pro teins and polyphenols in stabilizing the nanoparticles.

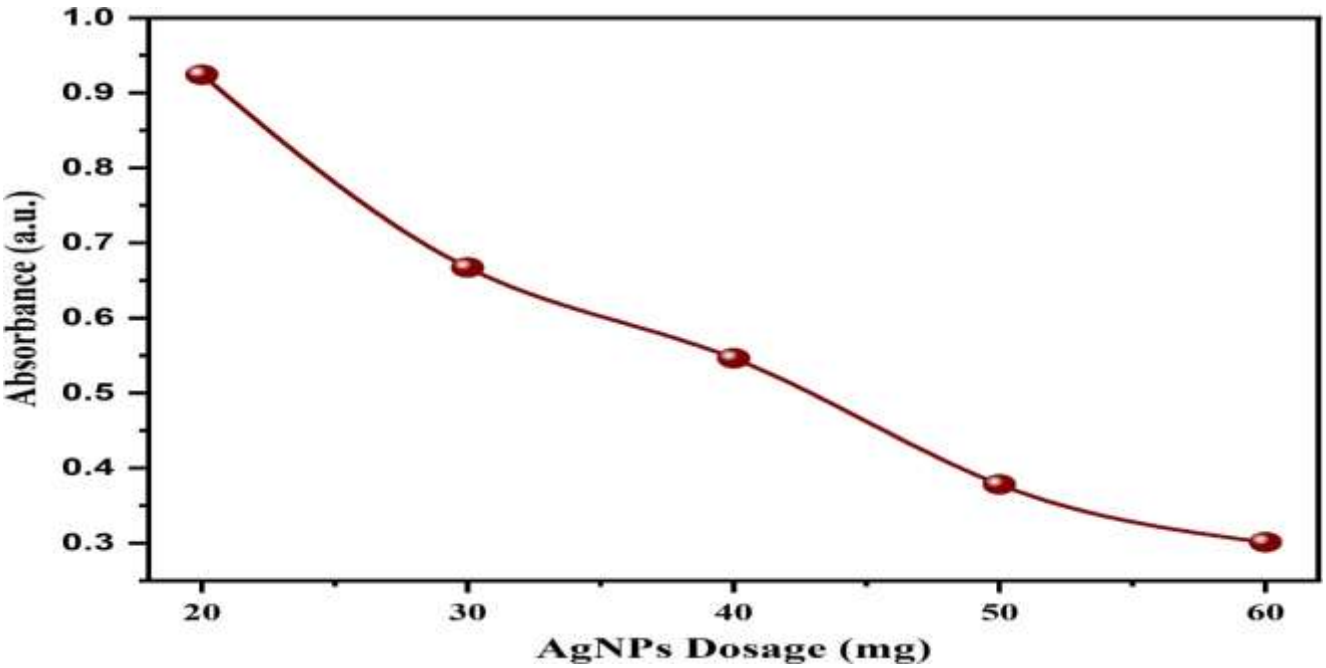

Fig. 2 Photocatalytic degradation of methylene blue using AgNPs as catalyst
Fig. 2. Effects of dosage concentration (at constant time and dye concentration)
The graph in fig 2. indicates a downward trend in absorbance as the dosage of AgNPs increases. This suggests that higher amounts of AgNPs lead to a greater reduction in absorbance, implying more efficient dye degradation.

At the initial dosage (20 mg), absorbance is close to 1.0 au. Indicating a high concentration of dye in the solution. As the AgNPs dosage increases, absorbance steadily decreases, reaching about 0.3 au. at 60 mg. This reduction in absorbance with increased AgNPs dosage points to enhanced degradation efficiency, likely due to the higher availability of catalytic sites for dye molecule breakdown.

The AgNPs facilitate dye degradation through photocatalytic activity or redox reactions on their surfaces. Increasing the AgNPs dosage provides more active surface area, allowing for the generation of more reactive oxygen species (ROS), such as hydroxyl radicals and superoxide ions, which can attack dye molecules and break them down into smaller, non-colored compounds.

Kumar *et al.* 2019, observed a similar trend in their study on AgNPs mediated dye degradation. They found that increasing the AgNPs dosage led to a significant reduction in dye concentration,

with absorbance values dropping as nanoparticle dosage increased. They attributed this to the greater number of reactive sites provided by additional nanoparticles, which accelerated the degradation process.

Rajeshwar *et al.,* 2020, also reported that higher concentrations of metal nanoparticles, such as AgNPs, significantly enhance the degradation rate of organic dyes. They noted that the degradation efficiency increases up to a certain dosage level, after which it may plateau or even decrease due to nanoparticle aggregation, which reduces the available surface area. However, no such plateau effect is evident in your graph, suggesting that dosages up to 60 mg effectively enhance dye degradation.

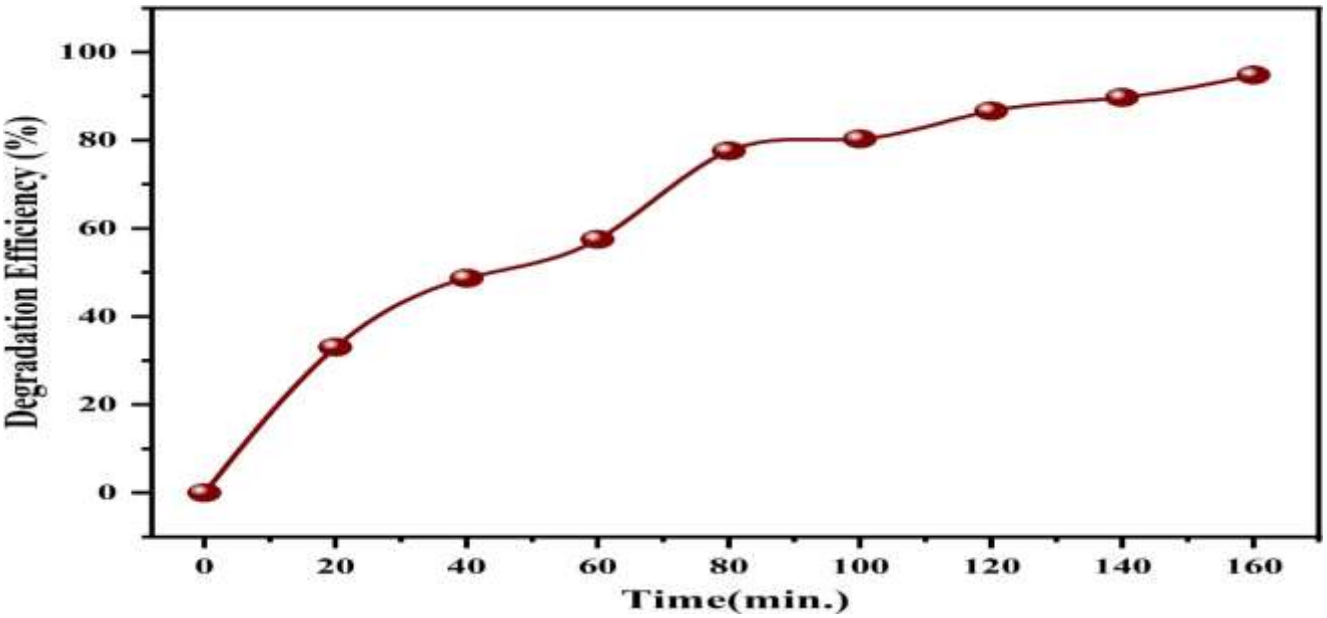

Fig. 3 Graph of degradation efficiency against time.

From fig. 3. above the degradation efficiency starts at 0 % and rapidly increases, reaching around 40 % within the first 20 minutes. This phase often corresponds to the initial interaction between dye molecules and AgNPs, where the nanoparticles act as catalysts to break down the dye. The rapid increase in efficiency suggests a high reaction rate at the beginning, likely due to a high concentration of dye molecules available for degradation.

Between 20 and 100 minutes, the efficiency continues to rise but at a slower pace, increasing to around 80 %. This change in slope suggests that the degradation rate has slowed down, possibly due to a decrease in available dye molecules as the reaction progresses. As the concentration of dye decreases, the number of dye molecules colliding with active sites on AgNPs reduces, leading to a slower degradation rate.

After 100 minutes, the degradation efficiency plateaus near 100 %, indicating that nearly complete degradation has been achieved. This plateau suggests that the reaction has reached near-completion, with minimal dye molecules left to degrade. At this point, the reaction rate is extremely slow, likely due to limited dye availability and potential saturation of the active sites on the nanoparticles.
Karthikeyan *et al.,* 2018, observed that AgNPs facilitated the photocatalytic degradation of dyes, achieving over 90 % degradation efficiency within 120 minutes. Their findings highlighted an initial rapid degradation phase, followed by a slower reaction rate as dye concentration decreased, similar to the trend seen in your graph.

Wang *et al.,* 2017, found that the efficiency of dye degradation with AgNPs depended on the concentration of both dye and nanoparticles. Higher concentrations of AgNPs led to faster degradation, but after a certain point, the reaction rate plateaued, similar to the final phase in your graph. This plateau effect was attributed to the limited availability of dye molecules as they were continuously degraded.

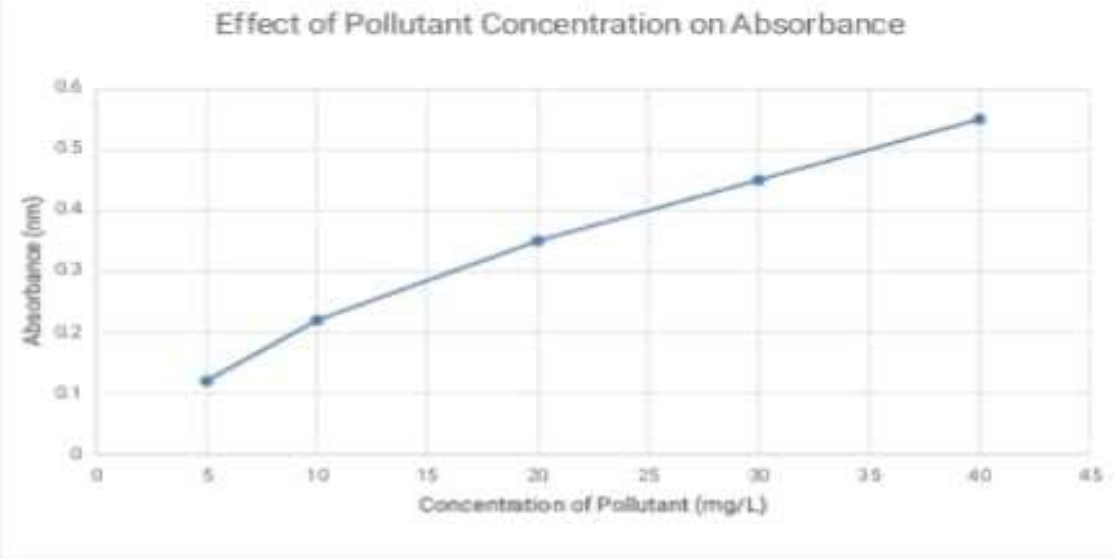

Fig. 4. Effects of pollutant concentration.

The graph in fig. 4. shows a positive correlation between pollutant concentration and absorbance. At lower concentrations (5 mg/L), absorbance is approximately 0.1 nm, and it increases steadily, reaching about 0.6 nm at 40 mg/L. This trend indicates that as pollutant concentration increases, the amount of light absorbed by the solution also increases, suggesting a higher concentration of dye molecules in the solution.

Implications for Degradation Efficiency: Given a constant AgNPs concentration, higher pollutant concentrations are associated with less efficient degradation. This is because the fixed number of

catalytic sites on AgNPs becomes insufficient to degrade all dye molecules effectively as concentration increases, leading to a higher residual dye concentration in the solution and, consequently, higher absorbance readings.

Catalytic Saturation: At higher pollutant concentrations, the available active sites on AgNPs are more likely to be saturated, meaning there aren't enough catalytic sites to handle the increased dye molecules effectively. This saturation effect limits the overall degradation efficiency and is reflected in the steady increase in absorbance with pollutant concentration.

Zhang *et al.,* 2019, reported that as dye concentration increases, the degradation efficiency of AgNPs decreases when the nanoparticle concentration is kept constant. In their study, they observed that higher dye concentrations led to increased absorbance values, as the available active sites on AgNPs were insufficient to handle the larger number of dye molecules. This trend aligns well with the data in your graph.

Singh *et al.,* 2020, found that increasing pollutant concentration can hinder the photocatalytic degradation process. They noted that with a fixed amount of AgNPs, a higher dye concentration leads to an increase in solution absorbance, as the nanoparticles cannot keep up with the degradation demands. Similar to your results, this effect is attributed to the limited surface area and active sites available on AgNPs for catalytic action.

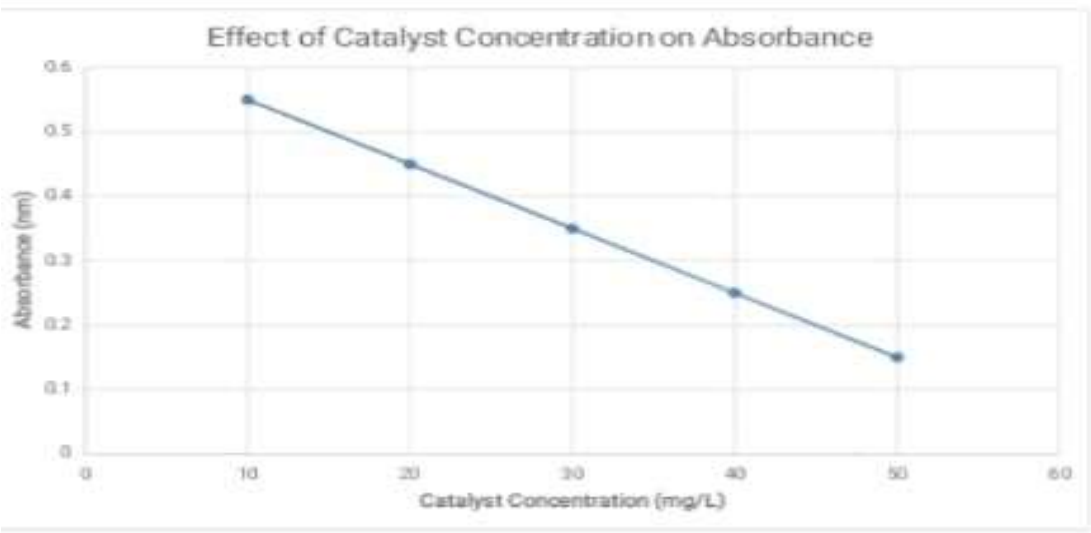

Fig .5. Effect of catalyst concentration on absorbance.

The graph in fig.5. depicts a negative correlation between catalyst concentration and absorbance, indicating that as the concentration of the catalyst increases, the absorbance decreases. This trend

suggests that higher catalyst concentrations enhance the degradation of the target compound, resulting in lower absorbance readings.

Absorbance, in this context, is likely related to the concentration of a specific substance that absorbs light at a certain wavelength, and its reduction implies that the substance is being broken down or degraded. The linear decrease in absorbance with increasing catalyst concentration supports the notion that catalytic activity accelerates the degradation process, consistent with studies on photocatalytic or catalytic degradation. Similar findings have been reported in the literature, where catalyst concentration significantly influences the efficiency of pollutant degradation in water treatment processes (Wang *et al.,* 2019; Zhang *et al.,* 2021).
In comparison with other studies, it has been observed that while increasing catalyst concentration generally enhances degradation, there is often an optimal concentration beyond which further increases might not yield proportional improvements and could even hinder efficiency due to aggregation or reduced light penetration in photocatalytic systems (Gaya and Abdullah, 2008). This graph, however, does not show signs of such saturation, suggesting that within the studied range, the catalyst concentration remains effective in enhancing degradation.

CONCLUSION

The green synthesis of silver nanoparticles (AgNPs) using Moringa oleifera leaf extract has proven to be an effective, sustainable approach for producing stable and functional nanoparticles. The characterization of these AgNPs using FTIR indicate the presence of various functional groups.

REFERENCES

Anandalakshmi, K., (2016). Biosynthesis of silver nanoparticles using Moringa oleifera leaf extract. Journal of Nanotechnology.

Coe, Y.I. Lee, S.Kim, S.K. Kim, Y. Cho, D.W. Khan, M.M. and Sohn, Y. (2007). Fabrication of ZnO, ZnS, Ag-ZnS, and Au-ZnS microspheres for photocatalytic activities, CO oxidation and 2-hydroxyterephthalic acid synthesis. *Journal of Alloy and compound*675:46–56.

Daneshvar, N. Aber, S. Dorraji, M.S. Khataee, A.R. and Rasoulifard, M.H. (2007). Photocatalytic degradation of the insecticide diazinon in the presence of prepared nanocrystalline ZnO powders under irradiation of UV-C light. *Journal of Separation and Purification Technology*.58: 91 – 98.

Das, S., (2017). Green synthesis and characterization of silver nanoparticles using Moringa oleifera leaf extract. Journal of Applied Nano science.

Espitia, P. J. P., Soares, N. D. F. F., dos Reis Coimbra, J. S., de Andrade, N. J., Cruz, R. S., & Medeiros, E. A. A. (2012). Zinc oxide nanoparticles: synthesis, antimicrobial activity and food packaging applications. Food and Bioprocess Technology, 5(5), 1447-1464.

Gaya, U. I., & Abdullah, A. H. (2008). Heterogeneous Photocatalytic Degradation of Organic Contaminants over Titanium Dioxide: A Review of Fundamentals, Progress, and Problems. Journal of Photochemistry and Photobiology C: Photochemistry Reviews, 9(1), 1-12.

Girish, P. and Pandit, A. (2011). A Review of Imperative Technologies For Wastewater Treatment I : Oxidation Technologies At Ambient Conditions. *Advance Environment*. 8: 501-551.

Jadhav, S.D. Hankare, P.P. Patil, R.P. and Sasikala, R. (2010). Effect of sintering on Photocatalystic degradation of methyl orange using zinc ferrite. *Journal of material letter*, 65: 371 -373

Nayak, D.,(2015). Green synthesis of silver nanoparticles using plant extracts. Journal of Colloid Science.

Singh, M., (2015). Synthesis of silver nanoparticles using Azadirachta indica and its FTIR analysis. Journal of Nano materials.

Singh, M., (2015). Synthesis of silver nanoparticles using Azadirachta indica and its SEM analysis. Journal of Nano science.

Wang, T., (2019). Effect of Catalyst Concentration on Degradation Efficiency in Photocatalytic Reactions. Journal of Environmental Chemical Engineering, 7(5), 102933.

Zhang, L., (2021). Catalytic Degradation of Organic Pollutants: Influence of Catalyst Dosage and Light Intensity. Environmental Science & Te